Convection and convective-organization in hothouse climates

Guy Dagan[1], Jacob T. Seeley[2], and Nathan Steiger[1]

[1]Fredy and Nadine Herrmann Institute of Earth Sciences, Hebrew University, Jerusalem, Israel
[2]Department of Earth and Planetary Sciences, Harvard University, Cambridge, MA, USA

Key Points:

- We examine the temporal and spatial organization of convection in simulated hothouse conditions
- We show that the previously reported 'episodic deluge' precipitation regime does not operate synchronously throughout a large domain
- Episodic deluges still occur on smaller scales, even in the presence of convective self- or forced-aggregation

Corresponding author: Guy Dagan, guy.dagan@mail.huji.ac.il

Abstract

In a "hothouse" climate, very warm temperatures lead to a high tropospheric water vapor concentration. Sufficiently high water vapor levels lead to the closing of the water vapor infrared window, which prevents radiative cooling of the lower troposphere. Because water vapor also weakly absorbs solar radiation, hothouse climates feature radiative heating of the lower troposphere. In recent work, this radiative heating was shown to trigger a shift into a novel "episodic deluge" precipitation regime, where rainfall occurs in short, intense outbursts separated by multi-day dry spells. However, it is unclear whether these oscillations operate on larger scales and how these oscillations, which represent "temporal" convective self-organization, would manifest in the presence of traditional "spatial" self- or forced-aggregation in large-domain convection-permitting simulations. Here we conduct radiative-convective-equilibrium simulations of different domain sizes and geometries under hothouse conditions. We find that the temporal oscillations cannot operate synchronously throughout a large domain ($\mathcal{O}$ 1000 km), as gravity waves cannot propagate fast enough to synchronize the entire domain. We propose a measure for the degree of domain synchronization and show that it decreases with domain size. We also show that even in the presence of tropical convective self-aggregation, the temporal oscillations dominate local spatial-temporal rainfall distribution. Finally, we demonstrate that even when an idealized large-scale overturning circulation is present, the oscillatory regime dominates the local rainfall distribution. These results could have important implications for extreme precipitation event under warming climate.

Plain Language Summary

Water vapor is a strong greenhouse gas that closely follows surface temperature. In a "hothouse" climate, temperature and water vapor are sufficiently high that the water vapor infrared window closes off, resulting in radiative heating of the lower troposphere. This was recently shown to causes rainfall to occur in short, intense outbursts, separated by multi-day dry spells. However, it is unclear whether these oscillations occur on larger scales and what their characteristic scale is. In this study, radiative-convective-equilibrium simulations were conducted to address these uncertainties. The simulations showed that the oscillations cannot occur synchronously throughout a large domain, as gravity waves cannot propagate fast enough to synchronize the entire domain. However, even in a large domain which include convective self-aggregation, the temporal oscillations dominate local spatial-temporal rainfall distribution.

1 Introduction

Earth's climate history includes extremely warm, ice-free states known as "hothouse" climates (Sleep, 2010; Charnay et al., 2017; Meckler et al., 2022). In addition, in the future, as the Sun's luminosity increases with its stellar evolution on the main sequence, Earth's climate is anticipated to transition into hothouse conditions before reaching a runaway greenhouse state (Wolf & Toon, 2015; Seeley & Wordsworth, 2021). Under such hothouse conditions, the water vapor concentration in the lower troposphere is expected to be sufficiently high that the water vapor infrared window would become opaque (Wolf & Toon, 2015; kumar Kopparapu et al., 2016; Popp et al., 2016; Wolf et al., 2018; Seeley & Wordsworth, 2021). Once the water vapor infrared window is closed, the lower-tropospheric radiative cooling that is observed under current climate conditions is anticipated to shift to radiative warming, driven by a lack of longwave cooling and a weak shortwave absorption by water vapor (Wolf et al., 2018; Seeley & Wordsworth, 2021). Previously it was shown that this lower-tropospheric radiative heating (LTRH) could lead to convective inhibition, thus significantly affecting the behavior of convection (Wolf et al., 2018; Seeley & Wordsworth, 2021). Recently a convection-resolving modelling study of the hothouse regime indicates that the LTRH drives a shift of the hydrological cycle

into a fundamentally different climate state: the "episodic deluge" or "relaxation oscillator" regime where short and intense outbursts of rainfall are separated by multi-day dry spells (Seeley & Wordsworth, 2021, hereafter SW21). Based on these results, SW21 suggested that a novel form of temporal convective self-organization may exist, and maybe even dominate, hothouse climates. SW21 speculated that this behaviour may have important implications for geological erosion processes.

The work of SW21 was based on small-domain radiative-convective-equilibrium (RCE) simulations (Wing, Reed, et al., 2018), which are known to prohibit more traditional spatial convective self-organization (or self-aggregation) (Muller & Held, 2012; Wing, Reed, et al., 2018). Convective self-aggregation, in its traditional definition, occurs when convection tends to cluster without an external forcing, such as from sea-surface temperature (SST) gradients (Muller & Held, 2012; Coppin & Bony, 2015; Wing, Emanuel, et al., 2018; Muller et al., 2022). Convective self-aggregation commonly appears in RCE simulations of global simulations with parameterized convection as well as in high resolution convection-permitting simulations (i.e., using few km resolution) when the domain size is large enough (Muller & Held, 2012; Wing et al., 2020; Muller et al., 2022). Convective self-aggregation is known to have a significant effect on the mean simulated climate conditions. For example, when convection aggregates under current climate conditions there is domain-mean drying, free-tropospheric warming, and more longwave radiation that is emitted to space (Bretherton et al., 2005; Muller & Held, 2012; Wing et al., 2020). In addition, convective self-aggregation was shown to increase the horizontal moisture variability and to be accompanied by the formation of dry patches with enhanced outgoing longwave radiation (Wing & Emanuel, 2014). The reduced humidity of the dry patches in an aggregated state should reduce the magnitude of LTRH at a given surface temperature (as compared to a disorganized state), and therefore might delay or prevent the emergence of the relaxation oscillator regime.

While the mechanisms responsible for triggering and maintaining self-aggregation are still not fully understood, it has been shown that interactions between longwave radiation and moisture are essential (Muller & Held, 2012; Coppin & Bony, 2015; Yang, 2018; Dingley et al., 2021). This longwave-moisture mechanism is driven by a strong clear-sky longwave radiative cooling in the dry parts of the domain, which, due to weak-temperature gradient approximation (Sobel et al., 2001), produces subsidence in these dry regions and acts to develop an overturning circulation. This circulation advects moist-static energy up-gradient to the moist convective-aggregated areas (Muller & Held, 2012). Due to the central role of the above feedback, it was shown that prescribing the radiative cooling rates (rather than letting them evolve as a function of the local water vapor concentration) can prevent convective self-aggregation (Muller & Held, 2012; Dingley et al., 2021).

In addition to spontaneously self-aggregating, convection can also be "forced" to aggregate by an SST gradient (Müller & Hohenegger, 2020; Hohenegger & Jakob, 2020; Lutsko & Cronin, 2021). In idealized "mock Walker" simulations, a simple SST gradient is imposed, forcing a large-scale overturning circulation (Grabowski et al., 2000; Bretherton et al., 2006; Lutsko & Cronin, 2021). Convection is then highly coupled to this large-scale overturning circulation (Bony et al., 2015).

A central unanswered question from SW21 is regarding the natural physical scale of the synchronized convective regime. In other words, would a simulation conducted in a larger domain produce similar oscillatory behaviour as reported in SW21? In this paper we aim at answering this question and at examining the potential effect of convective self- and forced-aggregation on the SW21's oscillatory behaviour.

2 Materials and Methods

Radiative-convective-equilibrium (RCE) simulations are conducted using the System for Atmospheric Modeling (Khairoutdinov & Randall, 2003, SAM) version 6.11.7, with its one-moment microphysical parameterization. Subgrid-scale fluxes are parameterized using Smagorinsky's eddy diffusivity model. In addition, gravity waves are damped at the top of the domain and doubly-periodic boundary conditions are assumed. These simulations generally follow the RCE Model Intercomparison Project (RCEMIP) protocol (Wing, Reed, et al., 2018) with some modifications as elaborated below.

Most of the simulations are conducted under spatially homogenized, prescribed SSTs (beside the mock Walker simulations – Table 1). The domain size is varied over a wide range of sizes and geometries. In addition, the horizontal resolution is also varied between 1 and 4.5 km (Table 1). In the vertical dimension, the grid is composed of 81 levels, which follows the RCEMIP protocol (Wing, Reed, et al., 2018) up to a height of 33 km and is extended to 40 km with 1 km resolution to account for the deeper troposphere under higher SSTs (Hartmann & Larson, 2002). A preindustrial level of CO_2 (280 ppm) is specified and the vertical profile of O_3's is as in Wing, Reed, et al. (2018). Other trace gases (such as CH_4 and N_2O) are neglected for simplicity.

A time step of up to 5s is used. Radiative fluxes are calculated every 5 minutes using the CAM (Community Atmosphere Model) radiation scheme (Collins et al., 2006), except for experiments using prescribed radiative cooling rates, see Table 1. The output resolution is 1 hour. Following Wing, Reed, et al. (2018), a net insolation close to the current climate tropical-mean value is set by fixing the incoming solar radiation at $551.58\,\mathrm{W\,m^{-2}}$, with a zenith angle of 42.05°. Small temperature perturbations ($\mathcal{O}$ 0.02 K) are added near the surface at the beginning of the simulation to initialize convection. The initial conditions for the simulations are based on the last 30-days of a 150-days long small domain (RCE_small, see Table 1) simulation for each SST value (Wing, Reed, et al., 2018). The rest of the simulations are run for 100 days (as in Wing, Reed, et al. (2018)) and the last 50 days of each simulation are used for the statistical analyses.

In addition to the simulations conducted under homogenized SST conditions, three additional "mock Walker" simulations (Grabowski et al., 2000; Bretherton et al., 2006; Lutsko & Cronin, 2021) are conducted with an SST gradient along the long dimension (X) of the domain and with a domain mean SST value of 325 K. The SST distribution is set as a sinusoidal function of X as presented in Fig. 10d-f. The SST range in this case is 5 K, which resembles the range observed over the tropical Pacific ocean (Lutsko & Cronin, 2021).

3 Results

Following the RCEMIP protocol, we start by comparing the domain mean rainfall time series in RCE_small and RCE_large simulations under the two different SSTs (Fig. 1). This figure demonstrates that the RCE_small simulations produce the oscillatory behaviour reported in SW21. This is specifically pronounced under the higher SST (325 K). However, the RCE_large simulations produces a very different domain mean rainfall, which is not episodic and regular; in the large domain simulations, on the entire domain scale, no short and intense outbursts are formed.

The RCEMIP protocol, which the simulations here follow, was designed in part to understand the effect of convective self-aggregation on the domain-mean properties (Wing, Reed, et al., 2018; Wing et al., 2020). This can be done by comparing the RCE_large and RCE_small simulations, and attributing the difference between them to the effect of convective self-aggregation alone (Wing et al., 2020). In our case, however, for attributing the difference between RCE_large and RCE_small to self-aggregation, we need to make sure that the RCE_large simulations are indeed aggregated in the traditional sense (as

Table 1. List of simulations

Simulation	SST [K]	Horizontal grid points	Resolution [km]	Interactive radiation
RCE_small_320	320	96×96	1	✓
RCE_small_325	325	96×96	1	✓
RCE_large_320	320	2048×128	3	✓
RCE_large_325	325	2048×128	3	✓
RCE_large_320_FixedRAD	320	2048×128	3	
RCE_large_325_FixedRAD	325	2048×128	3	
RCE_largeX2.25	325	2048×128	4.5	✓
RCE_large/2	325	1024×128	3	✓
RCE_large/4	325	512×128	3	✓
RCE_large/8	325	256×128	3	✓
RCE_large/18	325	256×128	2	✓
RCE_large/32	325	256×128	1.5	✓
RCE_large/72	325	256×128	1	✓
RCE_square_1	325	256×256	3	✓
RCE_square_2	325	128×128	3	✓
RCE_square_3	325	96×96	2	✓
mock_Walker_1	325	2048×128	3	✓
mock_Walker_2	325	2048×128	1.5	✓
mock_Walker_3	325	512×128	3	✓

opposed to its temporal form as suggested by SW21). In addition, in our case the difference between RCE_large and RCE_small could also be driven by other reasons beside self-aggregation. In particular, the difference in the domain-mean rainfall between RCE_large and RCE_small could also be driven by a difference in the level of synchronization of the simulations (caused solely by the different domain sizes even in the absence of self-aggregation).

To check if the RCE_large simulations are aggregated, we examine Hovmoller diagrams of the outgoing longwave radiation (OLR) and precipitable water of these simulations in Fig. 2. This figure shows that the RCE_large simulations do indeed feature dry patches with enhanced OLR, as produced by convective self-aggregation. As expected (Bretherton et al., 2005; Muller & Held, 2012; Wing et al., 2020), the formation of these dry patches with enhanced local OLR also produced an increased domain mean and maximum OLR compared with the unaggregated RCE_small simulations (Figs. S1 and S2, SI). In addition, we calculate a common metric for convective-aggregation, I_{org} (Tompkins & Semie, 2017, Fig. S3, SI), which also suggests that the large domain simulations are aggregated in the traditional sense (values well above 0.5). However, it is not immediately clear what I_{org} represents in the presence of the SW21's temporally oscillatory behaviour. Nevertheless, from Fig. 2 and Figs. S1 and S2, SI we can conclude that the RCE_large simulations are aggregated in the sense that they include large dry patches and hence an enhanced OLR compared with the RCE_small simulations.

As was hypothesized in the introduction, the enhanced OLR in the presence of convective self-aggregation in the RCE_large simulations could reduce the LTRH in these simulations compared with RCE_small simulations. This is confirmed by comparing the domain- and time-mean radaiative heating rate (RHR) vertical profiles of the different simulations, Fig. 3. This figure shows that indeed convective self-aggregation acts to weaken the LTRH, i.e., the maximum LTRH is lower and the layer in which the RHR is positive is shallower in RCE_large than in RCE_small.

To examine the role of the reduced LTRH in the RCE_large compared with the RCE_small simulations, and to separate it from the effect of the domain size alone, we re-ran the

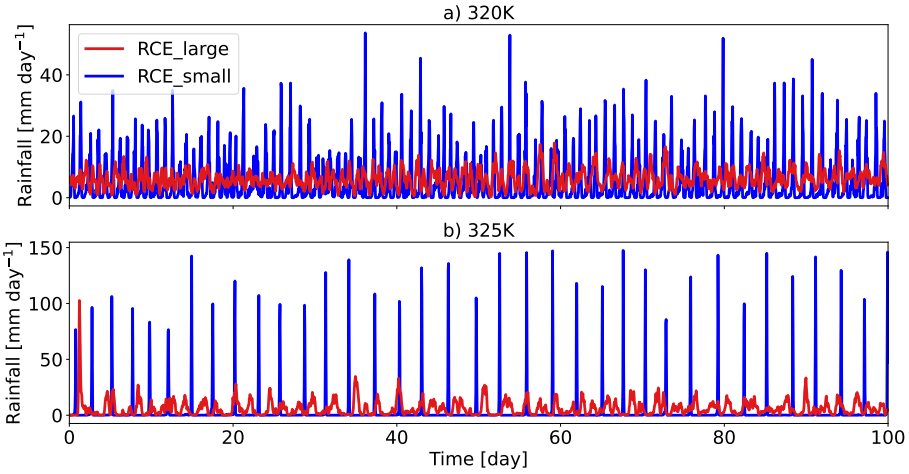

Figure 1. Domain mean rainfall time series in RCE_small and RCE_large simulations under SST of 320 K (a) and 325 K (b)

RCE_large simulations with a prescribed RHR vertical profile taken from the RCE_small simulations for each SST (RCE_large_FixedRAD). Prescribing the RHR vertical profile suppresses the formation of dry patches (see Fig. S4, SI), but this simulation still does not reproduce the strong oscillatory behaviour seen in RCE_small. Specifically, in Fig. 4 we compare the rainfall time series in RCE_large_FixedRAD with the RCE_small and RCE_large simulations. This figure demonstrates that domain-mean precipitation in RCE_large_FixedRAD is more similar to RCE_large than RCE_small.

Based on Fig. 4, we can conclude that the main difference between RCE_small and RCE_large is not due to the difference in convective self-aggregation and RHR vertical profile but rather related to the size of the domain, which affects the synchronization of the convection (as elaborated below).

To gain a better understanding of the distribution of rainfall in the RCE_large and RCE_large_FixedRAD simulations, we present Hovmoller diagrams of the rainfall in these simulations conducted under SST = 325 K in Fig. 5a and b (the Hovmoller diagrams for the simulations conducted under SST = 320 K are presented in Fig. S5, SI). It reveals that, while the domain mean rainfall in the large domain simulations does not exhibit short and intense outbursts, there are such outbursts in the rainfall on a local scale that cover only a portion of the domain. This means that averaging the rainfall over the entire domain masks strong oscillatory behavior that occurs on a more local scale.

Figure 5c-f provide a zoomed-in view of a representative rainfall outburst from each simulation (marked in red in Fig. 5a and b). The figure shows that the outburst begins at a specific location where large amounts of precipitable water accumulate. Once the rainfall starts, it spreads horizontally at a speed of around 60 km h^{-1}, which corresponds to the propagation speed of gravity waves. Typically, an outburst event lasts for approximately 12 hours (as shown in Fig. 5). With a propagation speed of 60 km h^{-1} in each direction for 12 hours, a typical rainfall event covers a distance of roughly 1500 km. Therefore, a typical event does not cover the entire domain, which has a length of over 6000 km.

Figure 5 indicates that convective self-aggregation, along with the formation of the associated dry patches, modulates the oscillatory behavior of SW21 and its spatial scales.

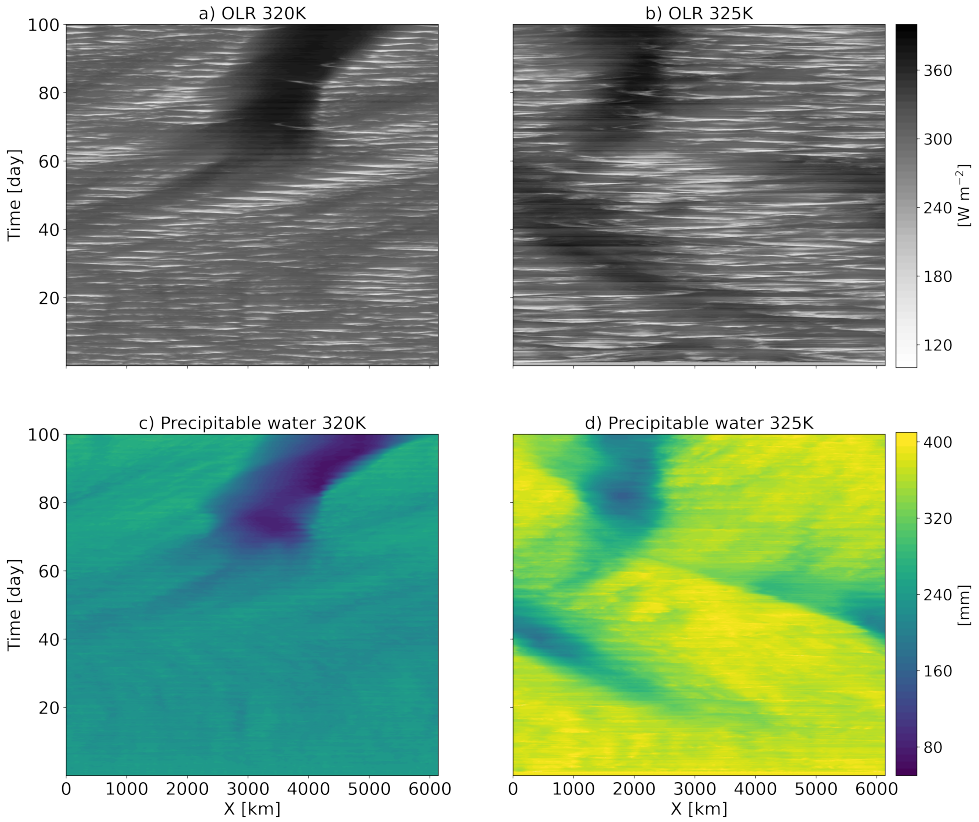

Figure 2. (a) and (b) Hovmoller diagrams of the TOA outgoing longwave radiaition (OLR). (c) and (d) Precipitable water for the two RCE_large simulations conducted under different SSTs, 320 K in (a) and (c), and 325 K in (b) and (d).

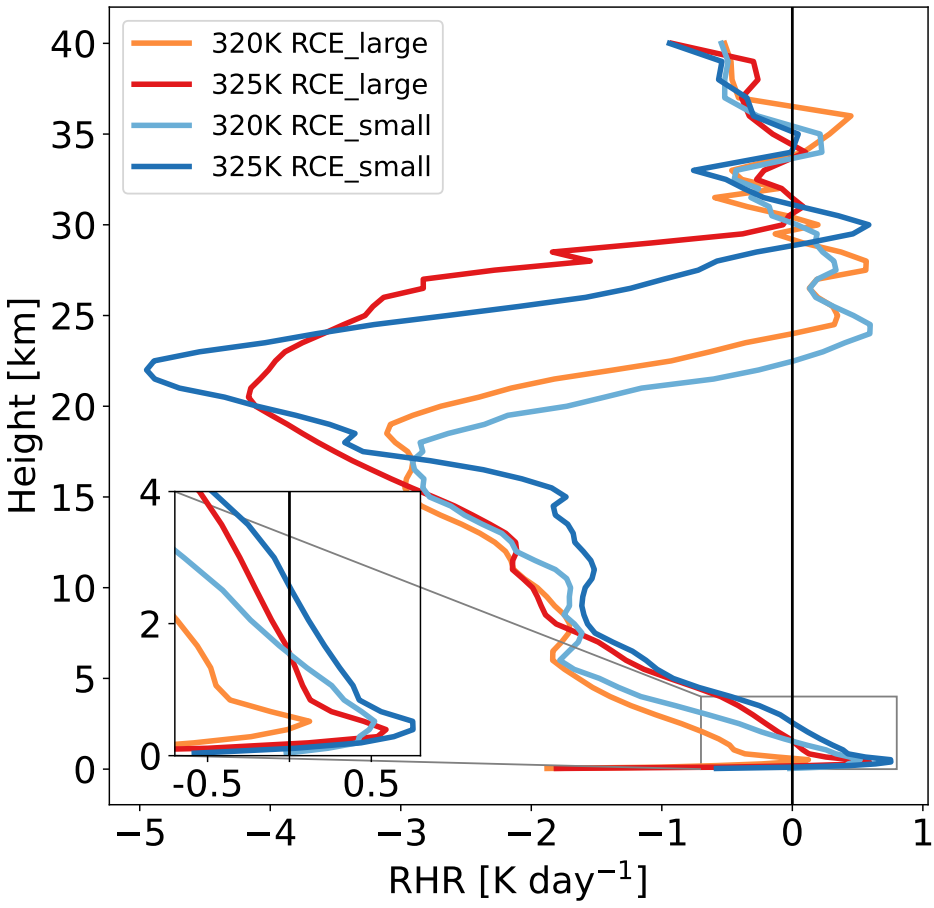

Figure 3. The domain- and time-mean (over the last 50-days of the simulations) radiative heating rate (RHR) vertical profiles of the RCE_large and RCE_small simulations conducted under different SSTs.

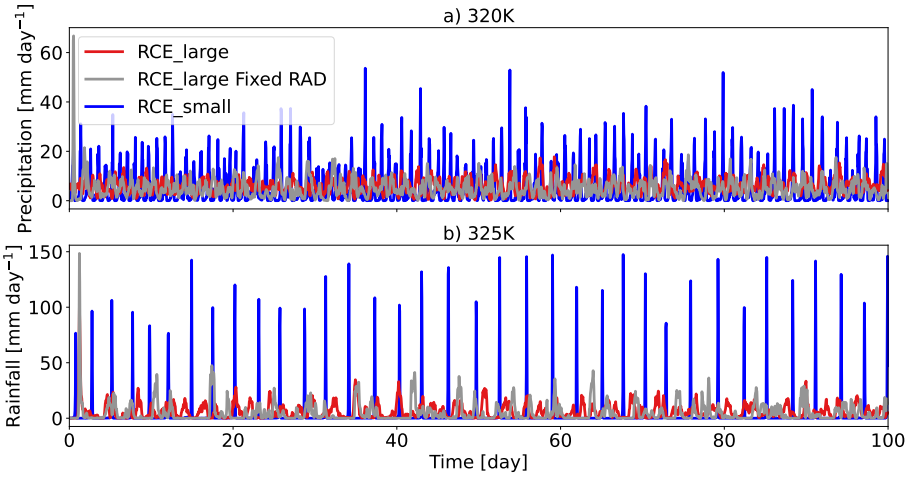

Figure 4. Domain mean rainfall time series in RCE_small, RCE_large and RCE_large_FixedRAD simulations under SST of 320 K (a) and 325 K (b)

This can be observed by comparing the RCE_large simulation, which includes dry patches, and the RCE_large_FixedRAD simulation, which does not. In particular, we note that these oscillations do not occur in the dry patches when interactive radiation is present; the large-scale moist patches in the aggregated state provide an "envelope" within which the oscillatory convective regime is embedded. Moreover, a propagating precipitating event that reaches a transition between wet and dry patches quickly evaporates (Fig. 5c and d). Hence, a characteristic localized outbursts is generally smaller in RCE_large than in RCE_large_FixedRAD simulations.

The conclusion from Fig. 4, that the main difference between RCE_small and RCE_large is not due to the difference in convective aggregation and RHR vertical profile but rather related to the size of the domain and the level of synchronization of the convection, invites examination of rainfall time series under a wide range of domain sizes (Table 1). Figure 6 illustrates that with the reduction in domain size the rainfall time series becomes more and more similar to the RCE_small simulation, trending toward distinct domain-mean rainfall outburst events separated by multiple dry days. That is to say that the rainfall becomes more synchronized throughout the domain as the domain size reduces.

The degree of rainfall synchronization throughout the domain can also be observed in the Hovmoller diagrams presented in Fig. 7. It demonstrates that rainfall events that propagate across the domain cover an increasingly larger fraction of the domain as the domain size decreases. In RCE_small domain, where a propagation speed of 60 km h^{-1} in each direction means that a rainfall event covers the entire domain in less than 1 hour (the output temporal resolution), the precipitation events are shaped like delta functions, as seen in Fig. 6.

To give a more quantitative measure of the degree of synchronization of the rainfall throughout the domain, in this paper we use the rainfall relative dispersion, η: the ratio of the standard deviation to the mean. High values of η represent a case in which the rainfall occurs mostly in short events with very high rates above the mean and long periods with no rain. Low values of η represent a steady regime of rainfall, with low standard deviations compared to the mean. The ability of η to capture the degree of rainfall synchronization throughout the domain is demonstrated in Fig. 8, which presents

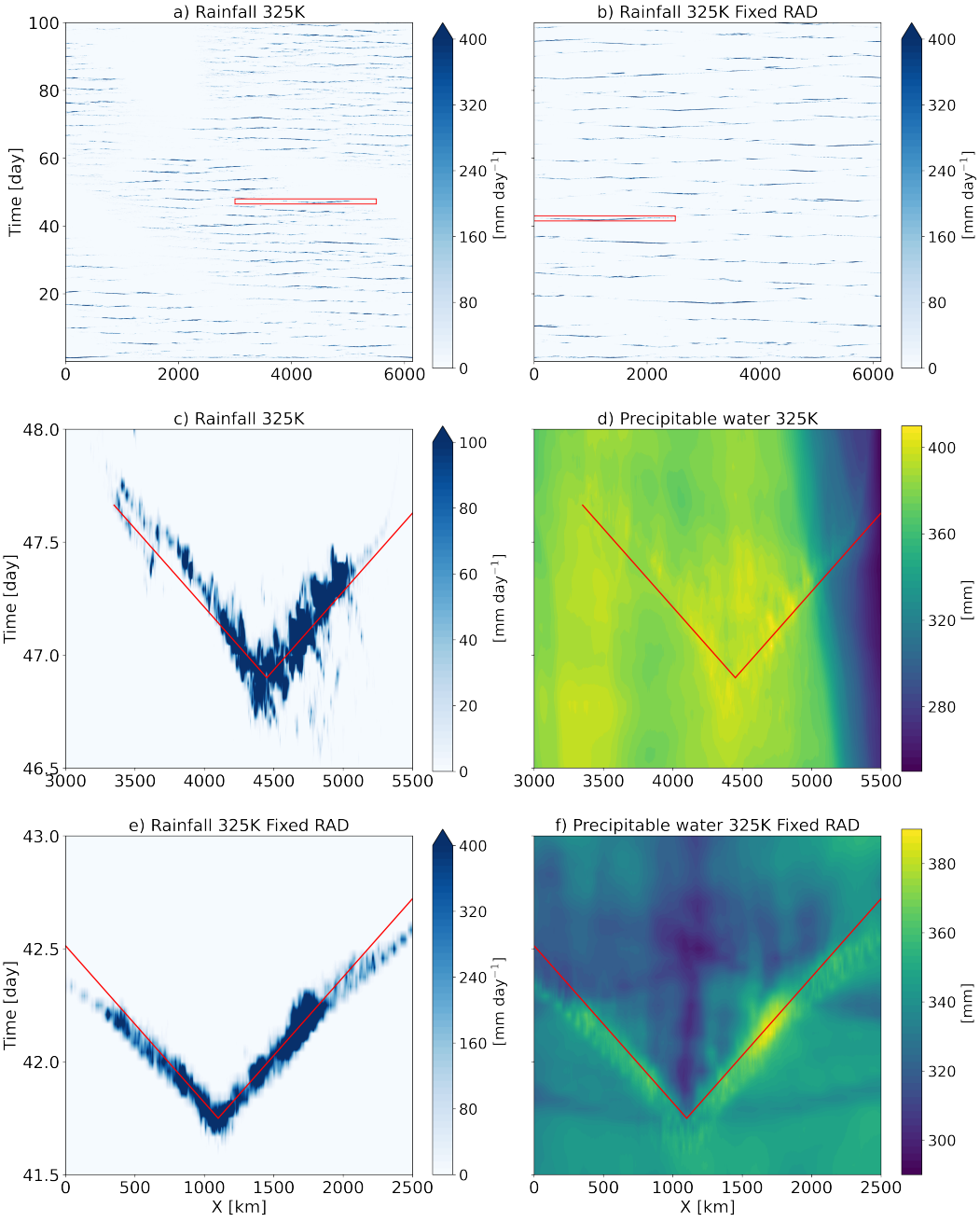

Figure 5. Hovmoller diagrams of the rainfall for RCE_large (a), and RCE_large_FixedRAD (b) simulations conducted under SST = 325 K. The red box in (a) isolates the rainfall event highlighted in (c) and (d), while the box in (b) isolates the rainfall event highlighted in (e) and (f). Red curves in c-f represent a propagation speed of 60 km h^{-1}.

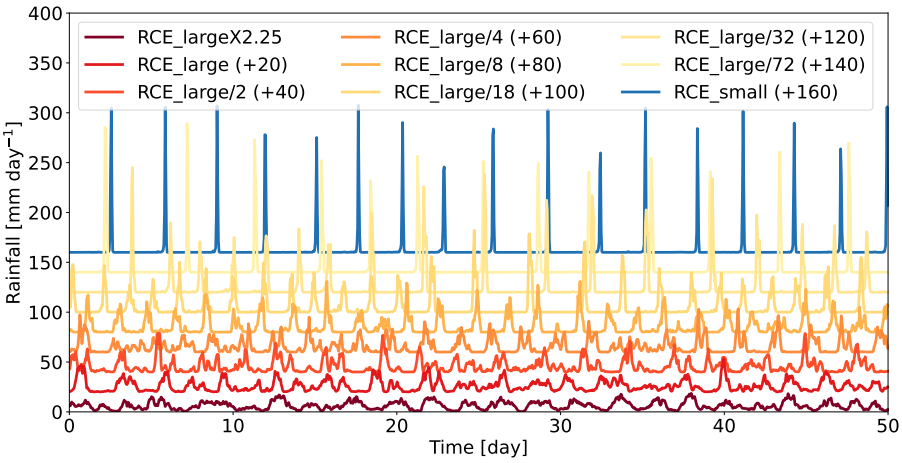

Figure 6. Domain mean rainfall time series for simulations conducted with SST = 325 K and with different domain sizes. For clarity a specific offset value has been added to each curve, as noted in the legend.

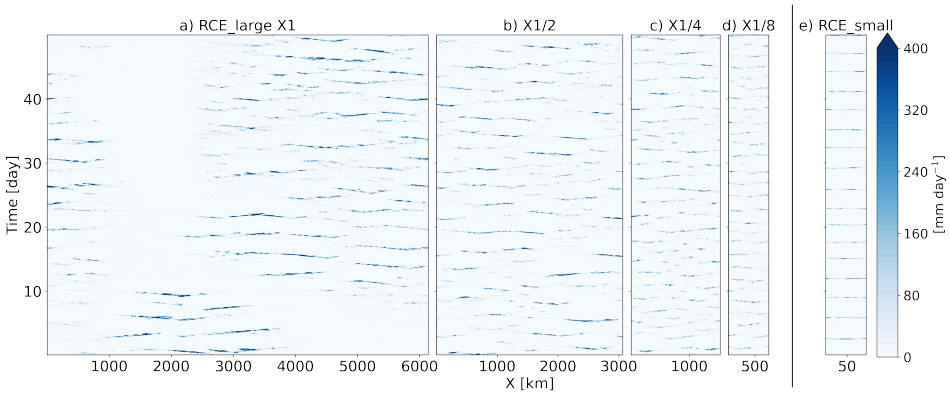

Figure 7. Hovmoller diagrams of the rainfall for simulations conducted with SST = 325 K and with different domain sizes, focused on the last 50 days of the simulations. Note that the RCE_small (e) simulation is not to scale with the rest of the simulations

the SST, domain mean rainfall and η from the slab ocean RCE simulation of SW21. Specifically, it demonstrates that η sharply increases from values below 1, when the SST is closer to our current climate conditions (305K), up to about 4–5 when the SST crosses the 325 K level.

Figure 9 presents η for all simulations conducted under homogeneous SST of 325 K (Table 1). It demonstrates that indeed η monotonically decreases with the domain size from roughly 5 to below 1; this is a similar range observed in the SW21 experiments shown in Fig. 8. This trend suggests a lower degree of synchronization for larger domains. In addition, the geometry of the domain (rectangle vs. square domains) could potentially have an effect on the propagation of the convection throughout the domain and hence on the degree of synchronization. To examine that, Fig. 9 presents three additional simulations (beside RCE_small) conducted with a square domain of different sizes (Table 1). It demonstrates that, at least for the cases examined here, the geometry of the domain does not affect the sensitivity of the degree of synchronization to domain size.

The simulations examined so far were conducted under homogeneous SST. Next we examine the three mock Walker simulations which were conducted under different domain sizes and resolutions (Table 1). Figure 10 demonstrates that even in the presence of SST-gradient forced large-scale circulation, short and intense outbursts of precipitation dominate the hydrological cycle. We note that these outbursts are concentrated around the center of the domain where the SST is warmest (Fig. S6, SI, presents the domain-mean rainfall time series of these simulations); this therefore verifies that the oscillator regime can be present within a tropical climate region only. In these simulations, which include large-scale circulation, there are persistent dry subsiding regimes present in the domain (at the two sides of the domain where the SST is lower than the domain mean). These persistent dry subsiding regimes act to enhance the longwave cooling of the atmosphere (Pierrehumbert, 1995, Fig. S7, SI), hence they act to weaken the domain-mean LTRH (Fig. S8, SI). Nevertheless, even this weak LTRH is enough to generate strong local rainfall oscillations (Fig. 10).

4 Conclusions

Hothouse climate conditions are believed to have existed in the history of our planet (Sleep, 2010; Charnay et al., 2017; Meckler et al., 2022) and they will very likely form in its distant future (Wolf & Toon, 2015; Seeley & Wordsworth, 2021). Under high greenhouse gas emissions, it is also possible that if Earth happens to have a high climate sensitivity then the temperatures examined in this paper could locally and occasionally appear even in the relatively near future (Saeed et al., 2021). Little is known concerning convection under these hot conditions, let alone about convective-aggregation.

In this paper, we have examined the claims of Seeley and Wordsworth (2021, SW21), which showed that under hothouse conditions convection shifts into a "relaxation oscillator" regime characterised by short and intense outbursts of rainfall separated by multi-day dry spells. The driver for this shift is the lower-tropospheric radiative heating (LTRH) that characterises hothouse conditions. SW21's conclusions were based on small domain simulations which prohibit "traditional" spatial convective self-aggregation (Muller & Held, 2012). Hence, it was unclear from SW21 what happens to this oscillatory behaviour when traditional self-aggregation is allowed in a larger domain or what the spatial scale is of the oscillations in SW21. To answer these questions we conducted a series of RCE simulations with different domain sizes and geometries under hothouse conditions (Table 1).

Comparing small and large domains, convection-permitting hothouse climate simulations demonstrate that SW21's oscillatory behaviour, which appears in small domain simulations, is not present in the spatial mean of large domain simulations. In addition,

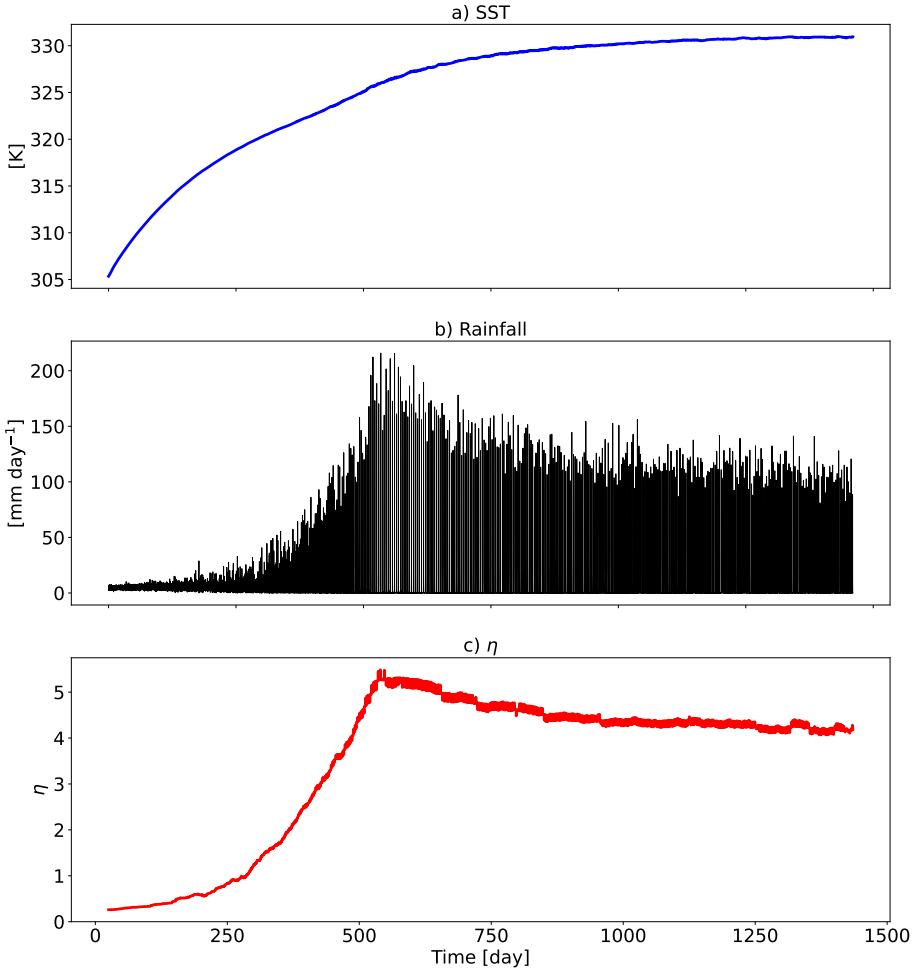

Figure 8. RCE simulation data from SW21: (a) The sea surface temperature (SST) and (b) the domain mean rainfall along with (c) the relative dispersion of the rainfall (η; defined as the ratio of the standard deviation to the mean) as a function of time. η is used here as a quantitative measure of the degree of synchronization of the rainfall throughout the domain and is calculated based on 50-days sliding window of the domain mean rainfall.

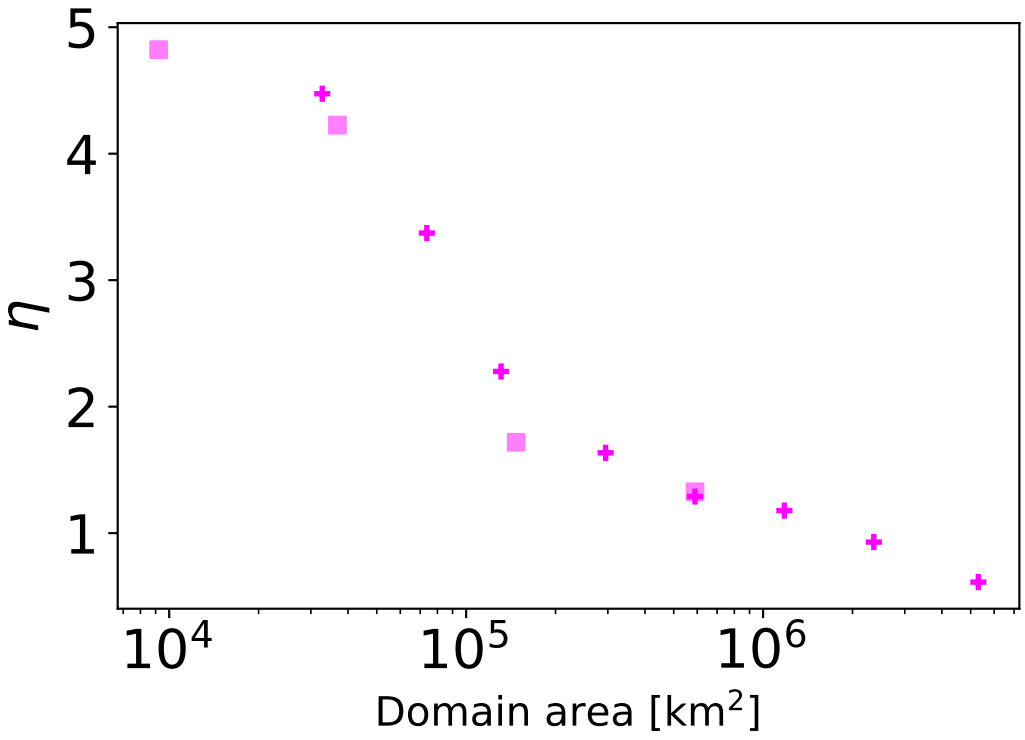

Figure 9. The relative dispersion of the rainfall (η; defined as the ratio of the standard deviation to the mean) for the different simulations conducted under homogeneous SST of 325 K. These results are based on the last 50 days of each simulation. η is used here as a quantitative measure of the degree of synchronization of the rainfall throughout the domain. Square markers represent square domain simulations, plus markers represent rectangle domain simulations

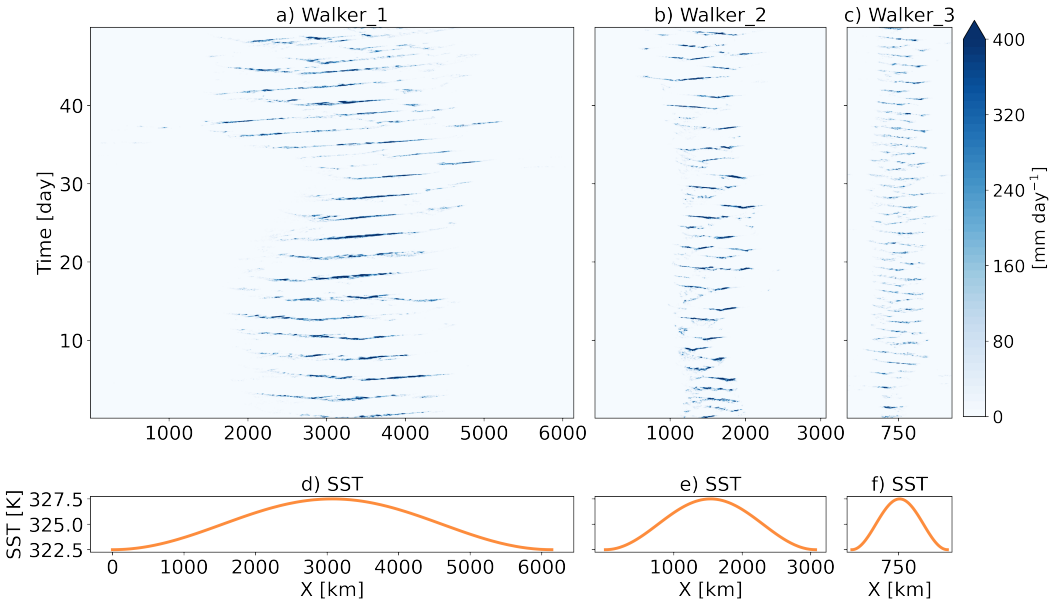

Figure 10. (a)-(c) Hovmoller diagrams of the rainfall for mock Walker simulations conducted with domain mean SST of 325 K and with different domain sizes, focused on the last 50 days of the simulations. (d)-(f) The prescribed SST spatial distribution along the long dimension of the domain (X).

these simulations demonstrate that "traditional" convective self-aggregation (Muller et al., 2022) is formed under hothouse conditions when the domain is large enough to allow it (Muller & Held, 2012). Similarly to our current climate conditions, convective self-aggregation in hothouse climates dries the atmosphere, enhancing the outgoing longwave radiation and weakening the LTRH. However, large-domain simulations with prescribed radiative heating rates demonstrate that preventing convective self-aggregation and its dampening effect on the LTRH does not bring the large-domain simulations back to the oscillatory behaviour seen in the small domain simulations. Hence, we conclude that while convective self-aggregation modulates the spatial distribution of convection in hothouse climates, it cannot explain the difference seen between small and large domain simulations. Instead, we demonstrate that the degree of synchronization of the convection throughout the domain decreases with the domain size. More specifically, we suggest that gravity waves are responsible for the synchronization of the convection. The propagation speed of the gravity waves (which is a few 10's km h^{-1}) and the domain size, determine the degree of synchronization, which can be measured by the domain mean rainfall relative dispersion (ratio of standard deviation to mean).

In addition, we examine the effect of an idealized SST-forced large-scale circulation on the SW21's oscillatory behaviour in mock-Walker simulations with different domain sizes. The imposed large-scale circulation forces the convection to aggregate along the regions of higher SST. However, we have demonstrated that the convection still occurs in short and intense outbursts even in the presence of large-scale circulation. These outburst events occur despite the fact that the presence of large-scale circulation acts to weaken the LTRH by enhancing the outgoing longwave radiation at the subsiding regions.

As noted in SW21, the oscillatory behaviour have analogs in our current climate conditions. Specifically, temporal oscillations in convection have been reported for deep

convective clouds (Yano & Plant, 2012), shallow convective clouds (Dagan et al., 2018) and even marine strato-cumulus clouds (Feingold et al., 2010). In the former two cases (deep and shallow convection), cycles of recharge-discharge of thermodynamic instability were identified (Bladé & Hartmann, 1993; Yano & Plant, 2012; Dagan et al., 2018). The mechanism behind these oscillations is as follows: once sufficient convective available potential energy accumulates in the atmosphere, convection initiate and act to consume the instability, until the convection stops. Next the instability builds up again by surface fluxes and radiative cooling, until launching another cycle (Yano & Plant, 2012; Dagan et al., 2018). The addition of the LTRH under hothouse conditions could strongly intensify the strength of these oscillations and make them dominate the local precipitation distribution. In addition, under hothouse conditions an additional mechanism, as proposed by SW21 is in play (involving the formation of virga and associated evaporative cooling that triggers an outburst). Hence, based on the results presented here, we speculate that under extreme global warming scenarios, an oscillatory behaviour will become more pronounced in the warmest parts of the globe, which could have strong implications for extreme precipitation (Knapp et al., 2008; Pendergrass, 2018).

5 Open Research

The model SAM is publicly available at: `http://rossby.msrc.sunysb.edu/marat/SAM.html`. The data presented in this study is publicly available at: `https://doi.org/10.5281/zenodo.7817396`.

Acknowledgments

This research has been supported by the Israel Science Foundation (grant no. 1419/21). We thank Yonatan Goldsmith for very fruitful discussions during the preparation of this paper.

References

Bladé, I., & Hartmann, D. L. (1993). Tropical intraseasonal oscillations in a simple nonlinear model. *Journal of Atmospheric Sciences*, *50*(17), 2922–2939.

Bony, S., Stevens, B., Frierson, D. M., Jakob, C., Kageyama, M., Pincus, R., ... others (2015). Clouds, circulation and climate sensitivity. *Nature Geoscience*, *8*(4), 261–268.

Bretherton, C. S., Blossey, P. N., & Khairoutdinov, M. (2005). An energy-balance analysis of deep convective self-aggregation above uniform sst. *Journal of the atmospheric sciences*, *62*(12), 4273–4292.

Bretherton, C. S., Blossey, P. N., & Peters, M. E. (2006). Interpretation of simple and cloud-resolving simulations of moist convection–radiation interaction with a mock-walker circulation. *Theoretical and Computational Fluid Dynamics*, *20*(5), 421–442.

Charnay, B., Le Hir, G., Fluteau, F., Forget, F., & Catling, D. C. (2017). A warm or a cold early earth? new insights from a 3-d climate-carbon model. *Earth and Planetary Science Letters*, *474*, 97–109.

Collins, W. D., Rasch, P. J., Boville, B. A., Hack, J. J., McCaa, J. R., Williamson, D. L., ... Zhang, M. (2006). The formulation and atmospheric simulation of the community atmosphere model version 3 (cam3). *Journal of Climate*, *19*(11), 2144–2161.

Coppin, D., & Bony, S. (2015). Physical mechanisms controlling the initiation of convective self-aggregation in a general circulation model. *Journal of Advances in Modeling Earth Systems*, *7*(4), 2060–2078.

Dagan, G., Koren, I., Kostinski, A., & Altaratz, O. (2018). Organization and oscillations in simulated shallow convective clouds. *Journal of Advances in Modeling*

Earth Systems, *10*(9), 2287–2299.

Dingley, B., Dagan, G., & Stier, P. (2021). Forcing convection to aggregate using diabatic heating perturbations. *Journal of Advances in Modeling Earth Systems*, *13*(10), e2021MS002579.

Feingold, G., Koren, I., Wang, H., Xue, H., & Brewer, W. A. (2010). Precipitation-generated oscillations in open cellular cloud fields. *Nature*, *466*(7308), 849–852.

Grabowski, W. W., Yano, J.-I., & Moncrieff, M. W. (2000). Cloud resolving modeling of tropical circulations driven by large-scale sst gradients. *Journal of the atmospheric sciences*, *57*(13), 2022–2040.

Hartmann, D. L., & Larson, K. (2002). An important constraint on tropical cloud-climate feedback. *Geophysical research letters*, *29*(20), 12–1.

Hohenegger, C., & Jakob, C. (2020). A relationship between itcz organization and subtropical humidity. *Geophysical Research Letters*, *47*(16), e2020GL088515.

Khairoutdinov, M. F., & Randall, D. A. (2003). Cloud resolving modeling of the arm summer 1997 iop: Model formulation, results, uncertainties, and sensitivities. *Journal of the Atmospheric Sciences*, *60*(4), 607–625.

Knapp, A. K., Beier, C., Briske, D. D., Classen, A. T., Luo, Y., Reichstein, M., ... others (2008). Consequences of more extreme precipitation regimes for terrestrial ecosystems. *Bioscience*, *58*(9), 811–821.

kumar Kopparapu, R., Wolf, E. T., Haqq-Misra, J., Yang, J., Kasting, J. F., Meadows, V., ... Mahadevan, S. (2016). The inner edge of the habitable zone for synchronously rotating planets around low-mass stars using general circulation models. *The Astrophysical Journal*, *819*(1), 84.

Lutsko, N., & Cronin, T. W. (2021). Mean climate and circulation of mock-walker simulations. In *34th conference on hurricanes and tropical meteorology.*

Meckler, A. N., Sexton, P., Piasecki, A., Leutert, T., Marquardt, J., Ziegler, M., ... others (2022). Cenozoic evolution of deep ocean temperature from clumped isotope thermometry. *Science*, *377*(6601), 86–90.

Muller, C., & Held, I. M. (2012). Detailed investigation of the self-aggregation of convection in cloud-resolving simulations. *Journal of the Atmospheric Sciences*, *69*(8), 2551–2565.

Muller, C., Yang, D., Craig, G., Cronin, T., Fildier, B., Haerter, J. O., ... others (2022). Spontaneous aggregation of convective storms. *Annual Review of Fluid Mechanics*, *54*, 133–157.

Müller, S. K., & Hohenegger, C. (2020). Self-aggregation of convection in spatially varying sea surface temperatures. *Journal of Advances in Modeling Earth Systems*, *12*(1), e2019MS001698.

Pendergrass, A. G. (2018). What precipitation is extreme? *Science*, *360*(6393), 1072–1073.

Pierrehumbert, R. T. (1995). Thermostats, radiator fins, and the local runaway greenhouse. *Journal of the atmospheric sciences*, *52*(10), 1784–1806.

Popp, M., Schmidt, H., & Marotzke, J. (2016). Transition to a moist greenhouse with co2 and solar forcing. *Nature communications*, *7*(1), 10627.

Saeed, F., Schleussner, C.-F., & Ashfaq, M. (2021). Deadly heat stress to become commonplace across south asia already at 1.5 c of global warming. *Geophysical Research Letters*, *48*(7), e2020GL091191.

Seeley, J. T., & Wordsworth, R. D. (2021). Episodic deluges in simulated hothouse climates. *Nature*, *599*(7883), 74–79.

Sleep, N. H. (2010). The hadean-archaean environment. *Cold spring harbor perspectives in biology*, *2*(6), a002527.

Sobel, A. H., Nilsson, J., & Polvani, L. M. (2001). The weak temperature gradient approximation and balanced tropical moisture waves. *Journal of the atmospheric sciences*, *58*(23), 3650–3665.

Tompkins, A. M., & Semie, A. G. (2017). Organization of tropical convection in

low vertical wind shears: Role of updraft entrainment. *Journal of Advances in Modeling Earth Systems*, *9*(2), 1046–1068.

Wing, A. A., Emanuel, K., Holloway, C. E., & Muller, C. (2018). Convective self-aggregation in numerical simulations: A review. *Shallow clouds, water vapor, circulation, and climate sensitivity*, 1–25.

Wing, A. A., & Emanuel, K. A. (2014). Physical mechanisms controlling self-aggregation of convection in idealized numerical modeling simulations. *Journal of Advances in Modeling Earth Systems*, *6*(1), 59–74.

Wing, A. A., Reed, K. A., Satoh, M., Stevens, B., Bony, S., & Ohno, T. (2018). Radiative–convective equilibrium model intercomparison project. *Geoscientific Model Development*, *11*(2), 793–813.

Wing, A. A., Stauffer, C. L., Becker, T., Reed, K. A., Ahn, M.-S., Arnold, N. P., ... others (2020). Clouds and convective self-aggregation in a multimodel ensemble of radiative-convective equilibrium simulations. *Journal of advances in modeling earth systems*, *12*(9), e2020MS002138.

Wolf, E., Haqq-Misra, J., & Toon, O. (2018). Evaluating climate sensitivity to co2 across earth's history. *Journal of Geophysical Research: Atmospheres*, *123*(21), 11–861.

Wolf, E., & Toon, O. (2015). The evolution of habitable climates under the brightening sun. *Journal of Geophysical Research: Atmospheres*, *120*(12), 5775–5794.

Yang, D. (2018). Boundary layer diabatic processes, the virtual effect, and convective self-aggregation. *Journal of Advances in Modeling Earth Systems*, *10*(9), 2163–2176.

Yano, J.-I., & Plant, R. (2012). Finite departure from convective quasi-equilibrium: Periodic cycle and discharge–recharge mechanism. *Quarterly Journal of the Royal Meteorological Society*, *138*(664), 626–637.